# Heterogeneous N-Terminal Acylation of Retinal Proteins Results from the Retina's Unusual Lipid Metabolism

Grzegorz Bereta and Krzysztof Palczewski*

Department of Pharmacology, School of Medicine, Case Western Reserve University, Cleveland, Ohio 44106-4965, United States

Ⓢ *Supporting Information*

ABSTRACT: Protein N-myristoylation occurs by a covalent attachment of a C14:0 fatty acid to the N-terminal Gly residue. This reaction is catalyzed by a *N*-myristoyltransferase that uses myristoyl-coenzyme A as substrate. But proteins in the retina also undergo heterogeneous N-acylation with C14:2, C14:1, and C12:0 fatty acids. The basis and the role of this retina-specific phenomenon are poorly understood. We studied guanylate cyclase-activating protein 1 (GCAP1) as an example of retina-specific heterogeneously N-acylated protein. The types and the abundance of fatty acids bound to bovine retinal GCAP1 were C14:2, 37.0%; C14:0, 32.4%; C14:1, 22.3%; and C12:0, 8.3% as quantified by liquid chromatography coupled mass spectrometry. We also devised a method for N-acylating proteins *in vitro* and used it to modify GCAP1 with acyl moieties of different lengths. Analysis of these GCAPs both confirmed that N-terminal acylation of GCAP1 is critical for its high activity and proper Ca^{2+}-dependent response and revealed comparable functionality for GCAP1 with acyl moieties of various lengths. We also tested the hypothesis that retinal heterogeneous N-acylation results from retinal enrichment of unusual *N*-myristoyltransferase substrates. Thus, acyl-coenzyme A esters were purified from both bovine retina and brain and analyzed by liquid chromatography coupled mass spectrometry. Substantial differences in acyl-coenzyme A profiles between the retina and brain were detected. Importantly, the ratios of uncommon N-acylation substrates—C14:2- and C14:1-coenzyme A to C14:0-coenzyme A—were higher in the retina than in the brain. Thus, our results suggest that heterogeneous N-acylation, responsible for expansion of retinal proteome, reflects the unique character of retinal lipid metabolism. Additionally, we propose a new hypothesis explaining the physiological relevance of elevated retinal ratios of C14:2- and C14:1-coenzyme A to C14:0-coenzyme A.
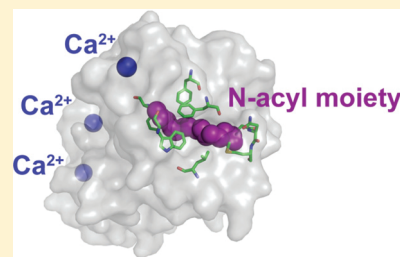
Co-translational modification of protein N-termini is widespread in nature. This process commonly involves removal of the initiation Met residue by a Met-aminopeptidase followed by covalent attachment of a two-carbon acetyl moiety by an N^{α}-terminal acyltransferase.[1,2] In cases when Met-aminopeptidase exposes Gly as the N-terminal residue, a 14-carbon myristoyl moiety can be covalently attached to its N-terminal amino group. This reaction is catalyzed by *N*-myristoyltransferase (NMT), which typically uses myristoyl-coenzyme A (C14:0-CoA) as a substrate. N-myristoylation usually promotes association with cell membranes, but other functions have also been proposed (reviewed in ref 3). Interestingly, retinal proteins have been found to be N-acylated with a unique set of fatty acids—dodecanoic (C12:0), *cis*-Δ5-tetradecenoic (C14:1n-9), and *cis,cis*-Δ5,Δ8-tetradecadienoic (C14:2n-6)—in addition to the typical tetradecanoic acid (C14:0) commonly known as myristoyl.[4–8] Such heterogeneous N-acylation was suggested to be retina-specific based on the following evidence: (i) the catalytic subunit of cAMP-dependent protein kinase (C-subunit of PKA) is heterogeneously acylated in the retina but not in the brain or heart;[7] (ii) analysis of N-linked fatty acids released from proteins of the retina, liver, and heart revealed the presence of C14:1 and C14:2 fatty acids exclusively in retinal samples.[9] The role of retinal heterogeneous N-acylation has thus far been studied for photoreceptor specific G protein, transducin, and

photoreceptor Ca^{2+}-binding protein, recoverin. The transducin results suggested that the acyl moiety of the α-subunit affects the strength of its interaction with the $\beta\gamma$-subunit.[4] The study of recoverin demonstrated that its potency as an inhibitor of light-dependent rhodopsin phosphorylation increases with the hydrophobicity of its acyl moiety.[10]

Guanylate cyclase-activating proteins (GCAPs) are Ca^{2+}-sensitive regulators of the photoreceptor membrane guanylate cyclases, GC1 and GC2.[8,11–14] GCAP2 probably also has other functions as suggested by its expression in synaptic terminals of photoreceptor cells.[15] However, GCAP1 may be of greater importance for human vision because of its association with a disease phenotype, namely cone—rod dystrophy.[16] As depicted in Figure 1A, the GCAP1 structure is characterized by a bilobal fold with two EF-hand motifs per lobe. All EF-hands except for N-terminal EF-hand 1 are capable of binding Ca^{2+}. The acyl moiety is located in a hydrophobic cavity (Figure 1B). Currently, most experimental data suggest that the acyl moiety remains in this cavity regardless of the Ca^{2+} concentration as opposed to GCAP's homologue, recoverin, where a Ca^{2+}-dependent myristoyl switch regulates reversible membrane binding.[17,18]
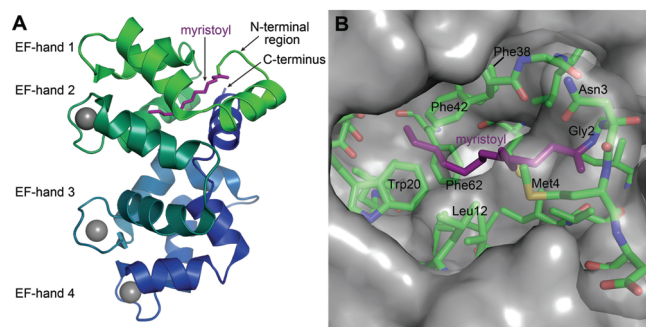
Figure 1. Crystal structure of myristoylated chicken GCAP1 with Ca^{2+} bound (PDB ID: 2R2I). (A) Cartoon representation of GCAP1 with Ca^{2+} shown as gray spheres, the myristoyl moiety as a purple stick, and polypeptide chain colors ranging from green (N-terminus) to blue (C-terminus). (B) Cavity occupied by the myristoyl moiety. Residues within 6 Å of the myristoyl moiety are shown as sticks. All labeled residues are identical in chicken, mouse, bovine, and human GCAP1. The figure was generated with PyMol v1.0.

Experiments carried out in the presence of lipids and GC1 are required to substantiate this model. Furthermore, GCAP1 has been shown to undergo heterogeneous N-acylation with C12:0, C14:2, and C14:1 in addition to the typical C14:0.[8] The relative abundance of these modifications in GCAP1 has not yet been established. Importantly, the effect of heterogeneous N-acylation on the activity and the Ca^{2+} sensitivity of GCAP1 has not been determined. A newly developed method for N-acylating proteins *in vitro* together with an accurate GC activity assay[19] allowed us to address this issue.

Why heterogeneous N-acylation of proteins is restricted to the retina has been investigated but not resolved.[20] Two major hypotheses have been considered. The first postulated that the retina contains a unique *N*-myristoyltransferase with broader fatty acyl-CoA substrate specificity, and the second suggested that the retinal CoA-pool is enriched with unusual NMT substrates. The first hypothesis was rejected because of the following findings: (i) only two NMT genes are present in the human genome, and both NMTs are ubiquitously expressed (reviewed in ref 3); (ii) although several NMT isoforms were reported, the same isoforms seem to be expressed in the retina and liver;[21] (iii) non-retinal cells overexpressing human NMT were capable of acylating recombinant protein if C14:1 and C14:2 were supplied in the growth media;[22] (iv) human NMT was shown to use C14:1 as substrate with a catalytic efficiency (V_{max}/K_{M}) only 1.9-fold lower than C14:0.[23] Evidence against the second hypothesis, which stated that the retinal CoA-pool is enriched in unusual NMT substrates, was provided in ref 9. Authors of this study tried to compare levels (using HPLC) of C12-, C14:1-, C14:2-, and C14:0-CoAs purified from retina, liver, and heart and obtained results implying that the retina is not enriched in these acyl-CoAs. However, authors of this difficult original work admitted to encountering some problems. The signal-to-noise ratio was low to the extent that peaks were sometimes hard to distinguish from background. Also, acyl-CoAs were identified by comparing their retention times with those of standards. Such an approach is not fully reliable for samples containing a complex acyl-CoA pool. For example, in our experience C14:1-CoA can exhibit a retention time identical to C16:3-CoA under certain separation conditions. Thus, omission of a C16:3-CoA standard, as in the above study, could lead to misrepresentation of the

C14:1-CoA level. Such reservations prompted us to confirm this study's findings before considering alternate hypotheses to explain the heterogeneous N-acylation. A technological advance from the previous approach was the use of MS for unambiguous identification of acyl-CoA species. Also, a more efficient method of acyl-CoA purification was recently described.[24] These improvements allowed analyses of retinal and brain acyl-CoAs with exceptional precision that led to our surprising findings.

Here, we report quantification of the N-acyl-GCAP1 variants in bovine retina. Furthermore, a new method of *in vitro* protein N-acylation is described that permitted attachment of acyl moieties of various lengths to the N-terminus of GCAP1. Our results confirm that N-acylation of GCAP1 is critical for its high activity and proper Ca^{2+} sensitivity and demonstrate that GCAP1 with acyl moieties of different lengths have similar functionality. Importantly, we discovered that the ratios of substrates for N-acylation—C14:2- and C14:1-CoA to C14:0-CoA—were higher in bovine retina relative to the brain. This relative enrichment of uncommon acyl-CoAs is suggested to be the major cause of heterogeneous N-acylation of GCAP1 and other retinal proteins. Other acyl-CoAs that were substantially elevated in the retina relative to the total acyl-CoA pool were C16:2, C18:2, C18:3 (precursor of long polyunsaturated fatty acids), C20:5, and C22:6 (DHA, required for retinal function). Furthermore, our data led us to formulate a hypothesis that the rare NMT substrates, C14:2- and C14:1-CoAs, are generated in the mitochondria due to a limited β-oxidation at the level of the long-chain fatty acid dehydrogenase.

■ EXPERIMENTAL PROCEDURES

Purification of GCAP1 from Bovine Retinas. The method for purifying bovine GCAP1 was adapted from a previously published procedure.[13] Bovine eyes were obtained from a local slaughterhouse. Retinas, removed from enucleated eyes, were stored at −80 °C, and all purification steps were performed at 4 °C. Sixty frozen retinas were fragmented with a mortar and pestle, resuspended in 60 mL of 10 mM HEPES, pH 7.4, with 25 μM leupeptin, and disrupted by sonication. To remove cell membranes, samples were centrifuged at 200000g for 1 h, and the resulting supernatant was recentrifuged under the same conditions. Meanwhile, G2G4-Sepharose resin containing the monoclonal anti-GCAP antibody G2G4 was equilibrated with 15 mL of 10 mM HEPES, pH 7.4. Purification was carried out by a hybrid batch/column procedure. First, the supernatant in 50 mL conical tubes was combined with 1.5 mL of compacted G2G4-Sepharose and mixed end-over-end on a rotator for 4 h. Next, the suspension was transferred to a column, and the supernatant was pumped out at 0.5 mL/min. The supernatant then was passed through the column again at the same flow rate. The column was washed with 22.5 mL of 10 mM HEPES, 200 mM NaCl, pH 7.4, followed by the same volume of 10 mM HEPES, pH 7.4. Protein was eluted with 100 mM glycine, pH 2.5, in 0.5 mL fractions that were collected in 150 μL aliquots of 1 M Tris, pH 8.4, and mixed. Fractions containing GCAP1 were identified by SDS-PAGE and combined. To remove antibody and other high molecular weight contaminants, the sample was passed through a 100 000 MWCO Amicon Ultra filter (Millipore, Billerica, MA) following the manufacturer's instructions. The effluent was saved while the retained mixture (250 μL) was transferred to a microtube, mixed with 750 μL of 8 M guanidine-HCl, and incubated at 95 °C for 10 min to release

GCAP1 from the contaminating antibody. After cooling, the sample was reprocessed with the same 100 000 MWCO Amicon Ultra filter, and both flow-through fractions were combined. Next, the sample was concentrated to 250 μL with a 10 000 MWCO Amicon Ultra filter. To remove salt and other low molecular weight contaminants, the sample was diluted with water and reprocessed with a 10 000 MWCO Amicon Ultra filter. This step was repeated once.

Tryptic Digestion of Bovine GCAP1. The GCAP1 sample (250 μL, 100—200 μg) was dried by SpeedVac, dissolved in 40 μL of 6 M guanidine-HCl buffered with 50 mM Tris-HCl, pH 8.0, and incubated at 95 °C for 15 min with intermittent vortexing. After cooling, the sample was diluted by addition of 270 μL of 50 mM Tris-HCl, pH 7.6, to lower the guanidine-HCl concentration to <1 M and transferred as 150 μL portions into HPLC insert vials. Trypsin (Princeton Separations, Adelphia, NJ) was reconstituted in ice-cold 50 mM ammonium bicarbonate, 1 mM CaCl$_2$, and then 20 μL (1 μg) was added to each sample. Digestion was carried out at 37 °C for 15 h.

LC/MS Analysis of Intact GCAP1. Intact GCAP1 separation and analyses were performed with an Agilent 1100 HPLC system (Agilent Technologies, Santa Clara, CA) equipped with a XBridge BEH300 C$_4$ column (2.1 mm i.d., 5 cm length, 3.5 μm particle diameter, 300 Å pore diameter) (Waters, Milford, MA) coupled to a Finnigan LXQ MS (Thermo Electron Corp., San Jose, CA). GCAP1 purified from bovine retinas was directly injected onto the column for LC/MS analysis with the first 5 min of the run diverted to waste. Recombinant GCAP1 was desalted first by chloroform—methanol precipitation as described in ref 25, with reagent volumes reduced for processing in microtubes. The dried protein pellet was redissolved in 25 μL of ice-cold 100% formic acid with vortex mixing and diluted 20-fold with cold water within 10 s after adding the acid to prevent protein formylation. Two solvents were used for HPLC. Both HPLC solvent A, water, and solvent B, acetonitrile, contained 0.1% formic acid. The following HPLC program was used for bovine GCAP1: 2% B for 2 min, 2—25% B within 1 min, 25—60% B within 35 min, 60—100% B within 15 min, 100% B for 15 min, 100—2% B within 1 min, and hold at 2% B for 6 min. For recombinant GCAP1 the sequence was 5% B for 2 min, 5—25% B within 1 min, 25—100% B within 45 min, hold at 100% B for 15 min, 100—5% B within 1 min, and hold at 5% B for 6 min. The flow rate was 0.25 mL/min, and the column was kept at 20 °C. The MS was equipped with an ESI source and operated in the positive ion mode. To obtain an optimal signal intensity for GCAP1, the transfer capillary temperature was set to 370 °C and sheath, auxiliary, and sweep gases were set to 30, 5, and 0, respectively. Other parameters were tuned automatically. MS spectra were acquired over the m/z range of 1000—1800 for bovine GCAP1 and 800—1800 for recombinant mouse GCAP1 (see below). Data were displayed with Xcalibur 2.0.7. software.

LC/MS Analysis of N-Terminal Peptides Obtained by Tryptic Digestion of Bovine GCAP1. These analyses were performed like those for intact GCAP1 with the following differences. The HPLC program was as follows: 10% B for 2 min, 10—100% B within 40 min, hold at 100% B for 5 min, 100—10% B within 1 min, and hold at 10% B for 6 min. The flow rate was 0.3 mL/min. The MS was tuned for maximum sensitivity to the octapeptide GARASVLS-NH$_2$, settings that worked well for the N-terminal peptides from GCAP1. MS spectra were acquired over the m/z range of 350—2000. Tandem mass spectra

(MS/MS) were acquired over the m/z range of 280—2000 for manually selected parent ions fragmented by using a collision energy of 35 (arbitrary units). Because the sample was not desalted, the HPLC effluent was diverted to waste for the first 5 min of the run.

Interpretation of MS Data for Intact Proteins. Intact proteins electrosprayed in a positive ion mode become multiply protonated (charged), and thus the MS spectrum of a single protein appears as a characteristic series of peaks. Manual calculation of the protein's MW from such complex spectra requires assignment of charge states to its ions represented by these spectral peaks. To assign charge (z_x) of ion "x", the following formula was used: $z_x = (y - 1)/(x - y)$, where "x" is the m/z value of any ion and "y" is the m/z value of the ion immediately preceding "x" in the same series. With charge states assigned, the protein's MW was calculated from the formula MW $= x \times z_x - z_x \times 1.008$. For improved accuracy, the protein's MW was calculated for multiple peaks and the average was taken. In some instances results were confirmed by deconvolution carried out with software, namely ProMass version 2.5 SR-1 (Thermo Electron Corp., San Jose, CA).

Extraction of Acyl-CoAs from Bovine Retinas and Brain. This protocol was adapted from a previously published procedure described in great detail.[24] Fifteen bovine retinas or 7 g of brain (cerebral region) under liquid nitrogen were powdered with a glass mortar, and the powder (~5 g) was transferred to a 50 mL conical tube. Following addition of 25 mL of acetonitrile: isopropanol (3:1, v:v) the suspension was sonicated four times for 20 s with intermittent incubations on ice. Next, 8.3 mL of 0.1 M KH$_2$PO$_4$, pH 6.7, was added followed by 30 s sonication and 5 s of vortexing. The resulting mixture was aliquoted into microtubes and centrifuged at 16000g for 5 min. The supernatant was collected in glass test tubes (4 mL per tube), 1 mL of glacial acetic acid was added to each tube, and the samples were vortexed and kept on ice. Next, five columns, each filled with 100 mg of 2-(2-pyridyl)ethyl resin (Supelco, Bellefonte, PA), were conditioned with 1 mL of acetonitrile:isopropanol:water:acetic acid (9:3:4:4, v:v:v:v) and after sample loading, washed with 1 mL of the same solution. Coenzymes were eluted with 2 mL of methanol with 250 mM ammonium formate (4:1, v:v). The eluate from each column was dried by SpeedVac and dissolved in 225 μL of acetonitrile:water (1:1, v:v) with 0.1% triethylamine (present in our HPLC solvents but not essential for acyl-CoA dissolution). The resulting sample was centrifuged for 5 min at 16000g, 4 °C, and 50 μL of the recovered supernatant was immediately injected for LC/MS analysis.

LC/MS Analysis of Acyl-CoAs. The HPLC and MS were the same as used for intact protein analyses. Coenzymes were separated on an XBridge C$_{18}$, 2.1 mm i.d., 100 mm length column (Waters, Milford, MA) by using water with 0.1% triethylamine (TEA) as solvent A and acetonitrile with 0.1% TEA as solvent B. The following HPLC program was used: 20% B for 2 min, 20—50% B within 30 min, 50—100% B within 10 min, hold at 100% B for 5 min, 100—20% B within 1 min, and hold at 20% B for 10 min. The MS was equipped with an ESI source and operated in the negative ion mode. The instrument was tuned for maximum sensitivity to C14:0-CoA in the presence of 40% solvent B. The transfer capillary temperature was set to 350 °C; sheath, auxiliary, and sweep gases were set to 40, 5, and 0, respectively, and other parameters were adjusted automatically. MS spectra were acquired over the m/z range of 400—1600. MS/ MS were acquired over a m/z range of 280—2000 for manually

selected parent ions fragmented by using a collision energy between 22 and 26 (arbitrary units).

Expression of Mouse GCAP1. The cDNA sequence encoding mouse GCAP1 was isolated by PCR from total retinal cDNA and cloned into pFastBacHT (Invitrogen, Carlsbad, CA) to generate pFBmGCAP1. The GCAP1 cDNA was inserted downstream of the vector's sequence encoding the His-tag and TEV protease cleavage site. The GCAP1's native initiation Met was removed so that the TEV cleavage of the recombinant protein would liberate GCAP1 with Gly2 at the N-terminus. The sequence of recombinant GCAP1 expressed from this vector is presented in Figure 5A. The pFBmGCAP1 vector then was used to generate baculovirus following the Bac-to-Bac protocol available from Invitrogen (Carlsbad, CA), except that a PrepEase Bac purification kit from USB (Cleveland, OH) was used for bacmid purification and a 5-fold upscaling of P1 and P2 baculovirus production. High Five insect cells were cultured in Express Five SFM medium (Invitrogen, Grand Island, NY) in 2 L baffled Erlenmeyer flasks, inside an incubator shaker set at 27 °C and 120 rpm. To express GCAP1, 250 mL of fresh medium and 5 mL of GCAP1-baculovirus were added to eight flasks, each containing 250 mL of cell suspension at 5 million cells/mL. Cells were collected 52 h later by a 20 min centrifugation at 300g, and each pellet obtained from 1 L of culture was resuspended in 25 mL of 50 mM HEPES, 270 mM KCl, 30 mM NaCl, pH 7.4, containing 1 pellet of EDTA-free protease inhibitors (Roche, Mannheim, Germany) before being frozen in liquid nitrogen and stored at −80 °C.

Purification of Mouse GCAP1. Insect cells from 1 L of culture were thawed and disrupted by sonication, and the suspension was clarified by successive centrifugations at 30000g for 30 min, 100000g for 30 min, and 100000g for 1 h at 4 °C. The supernatant was collected without the upper lipid layer, filtered through a 0.45 μm PVDF filter, and loaded onto a chromatography column. All chromatography buffers contained 50 mM HEPES, 270 mM KCl, and 30 mM NaCl. In addition, the wash and elution buffers contained 10 and 200 mM imidazole, respectively. The pH was adjusted to 7.0 for equilibration and wash buffers, while the elution buffer pH was set at 7.4. All buffers were cold, and the entire procedure was carried out in a cold room. A 15 mm diameter column was packed with 9−10 mL of TALON resin (Clontech, Mountain View, CA), and the following solutions were pumped through it: equilibration buffer (10 resin volumes at 2 mL/min), sample (∼50 mL at 1 mL/min), wash buffer (20 resin volumes at 2 mL min), and elution buffer (30 × 1 mL fractions at 1 mL/min). Eluted protein-rich fractions identified by a protein assay from Bio-Rad (Hercules, CA) were combined. 20 μg of TEV protease was added per mg of GCAP1, and samples were incubated at 10 °C overnight to cleave the His-tag. Complete removal of the His-tag was confirmed by SDS-PAGE. Finally, the buffer was changed to 50 mM HEPES, 90 mM KCl, 10 mM NaCl, pH 7.4, using 10 mL Zeba columns (Thermo Scientific, Rockford, IL), and 0.5 mL aliquots of GCAP1 were frozen by immersion in liquid nitrogen. 50 mg of purified mouse GCAP1 was obtained from 1 L of insect cell culture.

Expression and Purification of Yeast *N*-Myristoyltransferase (NMT). Yeast NMT1 with a N-terminal His-tag was expressed from pET30-NMT1 vector in Rosetta2(DE3)pLysS bacteria (Novagen). The pET30-NMT1 vector was generated using pET30B (Novagen) and pBB131, a yeast NMT1 encoding vector, which was a kind gift from Jeffrey Gordon (Washington University). Bacteria (6 L) were grown in an incubator shaker at

37 °C in LB media with 50 μg/mL kanamycin, 34 μg/mL chloramphenicol to an optical density at 600 nm (OD$_{600\,nm}$) of 0.25. Then the temperature was lowered to 30 °C, and once an OD$_{600\,nm}$ of 0.5 was reached, expression of NMT1 was induced with 0.5 mM (final concentration) IPTG. Six hours later, bacteria were harvested by a 20 min centrifugation at 10000g. Each pellet obtained from 1 L of culture was resuspended in 50 mM HEPES, 270 mM KCl, 30 mM NaCl, pH 7.4, and frozen in liquid nitrogen. Purification was the same as for GCAP1, with 4 mL of compacted TALON resin binding 60 mg of NMT1 obtained per each liter of culture. Postpurification MS analyses revealed that 10−15% of NMT copurified with its myristoyl-CoA substrate. Removal of prebound myristoyl-CoA was critical as our *in vitro* N-acylation method requires NMT1 in molar excess over GCAP1 and because the use of substrates other than myristoyl-CoA was desired. To obtain myristoyl-CoA-free NMT1, the enzyme was incubated for 1 h at 10 °C with an octapeptide substrate (GARASVLS-NH$_2$), described in ref 26, added at a 5-fold molar excess over NMT1. Then NMT1 was separated from excess octapeptide by Zeba desalting columns equilibrated with 50 mM HEPES, 90 mM KCl, 10 mM NaCl, pH 7.4, following the manufacturer's instructions. Finally, NMT1 was concentrated to 35 mg/mL by water pretreated Centriprep (Millipore, Billerica, MA), divided into 0.5 mL aliquots and frozen in liquid nitrogen.

***In Vitro* N-Acylation of Mouse GCAP1.** For this acylation, 1.5 mL of 35 mg/mL NMT1 was transferred to a glass tube followed by addition of 24.3 μL of 20 mM acyl-CoA. After thorough mixing, the sample was incubated for 1 h at 10 °C to permit enzyme−substrate complex formation. (Preincubation of enzyme with substrate was essential to prevent the substrate from depositing in hydrophobic clefts of the target protein.) Next, 1.25 mL of GCAP1 at 4.4 mg/mL was added, and thus the final molar ratio of NMT1:acyl-CoA:GCAP1 was 4:2:1. The sample was mixed and incubated for 24 h at 10 °C. (A prolonged incubation was needed for acylation with lauroyl-CoA, which proceeded slowly compared to acylation with myristoyl- and pentadecanoyl-CoAs.) A control sample with NMT and GCAP1 but lacking acyl-CoA was also prepared. After reactions were completed, His-tagged NMT was removed by passing samples through a column packed with 12 mL of compacted TALON resin and equilibrated with 50 mM HEPES, 90 mM KCl, 10 mM NaCl, pH 7.4. Acylated GCAPs were divided into aliquots, frozen in liquid nitrogen, and stored at −80 °C.

GC Activity Assays. Properties of GCAPs were evaluated for their ability to activate GC. GC assays were performed as described in refs 27 and 28. The following buffers and reagents were prepared in advance: assay buffer (150 mM HEPES, 270 mM KCl, 30 mM NaCl, 50 mM MgCl$_2$, 2.5 mM EGTA, pH 7.4), protein buffer (50 mM HEPES, 90 mM KCl, 10 mM NaCl, pH 7.4), nucleotide mix (10 mM GTP, pH 7.4, 100 μCi/mL [α-^{33}P]GTP), alumina buffer (200 mM Tris, 50 mM EDTA, pH 7.4), 5 mM 3-isobutyl-1-methylxanthine (IBMX) in water, 20 mM leupeptin, 0.4 M HCl, 0.5 mg/mL bovine serum albumin (BSA), solutions of CaCl$_2$ in water 0.34, 0.77, 1.33, 2.10, 2.96, 3.92, 4.23, 4.40, 5.03 mM, GCAPs (100 μM in protein buffer with 0.5 mg/mL BSA for dose-dependence experiments and 20 or 32 μM in protein buffer for Ca^{2+} sensitivity experiments). Also, frozen pellets of HEK-293 cells stably expressing mouse GC1 (6 million cells per pellet) were prepared. For dose-dependence experiments, a pellet of GC1 expressing cells was resuspended in 0.7 mL of protein buffer with 20 μM leupeptin

and cells were disrupted by a 10 s sonication. Next, 0.5 mL of cell suspension was combined with 0.5 mL of assay buffer, 0.5 mL of IBMX, and 0.25 mL of water. After thorough mixing, 35 μL aliquots of this solution were placed in microfuge tubes and combined with 10 μL of GCAPs serially diluted in protein buffer containing 0.5 mg/mL BSA. (BSA was included to ensure that acylated GCAPs did not adhere to plastic microtube surfaces.) Samples were mixed by pipetting and incubated for 10 min at 4 °C. 15 μL of 0.4 M HCl was added to three samples to inactivate GC1 and determine the assay's background noise. Next, 5 μL of nucleotide mix was added to all samples, which then were mixed by pipetting and placed in a 30 °C water bath for 10 min. Reactions were stopped by placing on ice and addition of 15 μL of 0.4 M HCl followed by brief vortexing and a 4 min centrifugation at 16000g. To separate substrate (GTP) from product (cGMP), 40 μL of each sample was transferred to tubes with alumina (to bind GTP) that had been suspended in 0.5 mL of alumina buffer, and the suspensions were vortexed for 8 min. After a 4 min centrifugation at 16000g, supernatants (0.3 mL) were transferred to scintillation vials filled with 3 mL of scintillation cocktail, and radioactivity was measured in a scintillation counter. For Ca^{2+}-sensitivity experiments, 0.5 mL of cell suspensions prepared as previously described were combined with 0.5 mL of assay buffer, 0.5 mL of 5 mM IBMX, and 0.5 mL of 20 μM GCAP1. 40 μL of this mixture was aliquoted into microfuge tubes, combined with 5 μL of various dilutions of $CaCl_2$, mixed by pipetting, and incubated at 4 °C for 10 min. From this point on assays were performed exactly as described for the dose dependence experiments. SigmaPlot v11.0 was used to analyze the resulting data.

■ RESULTS

GCAP1 from Bovine Retina Is N-Terminally Modified, Primarily with 14-Carbon Fatty Acids. We previously reported that bovine GCAP1 is N-terminally acylated with C14:0, C14:1, C14:2, and C12:0 fatty acids.[8] Here, we sought to confirm these findings and determine the relative quantities of acylated products by performing an extensive LC/MS analysis of GCAP1 purified from bovine retinas. The LC/MS chromatogram of our GCAP1 preparation displayed a single major peak (Figure 2A), and its corresponding MS spectrum consisted of a series of peaks representing charge states of an individual protein (Figure 2B). The MW of this protein as calculated from the spectra (see Experimental Procedures) was 23 587 Da, which is close to the theoretical MW for C14:0-GCAP1 (23 589 Da). The 2 Da difference is consistent with GCAP1 modified with the unsaturated 14-carbon fatty acids in addition to the myristoyl. The resolution of our instrument (0.2 Da) did not allow these GCAP1 acylated variants to be distinguished by intact protein analysis. But upon closer inspection of the MS spectrum in Figure 2B, an additional, low abundance, acylated GCAP1 variant became evident (Figure 2C). Its calculated MW (23 561 Da) was the same as the theoretical MW for C12:0-GCAP1. Quantification of the areas under the MS spectral peaks revealed that C14-GCAP1 variants constituted 91.5 ± 0.3% of the total while C12-GCAP1 comprised only 8.5 ± 0.3%. Because acylated GCAP1 variants that differ only by the degree of saturation of their acyl moieties could not be distinguished by the intact protein approach, we analyzed tryptic peptides of GCAP1 as well. To ensure that the ratios of various acyl peptides were not altered during sample preparation, GCAP1 was digested in a HPLC glass
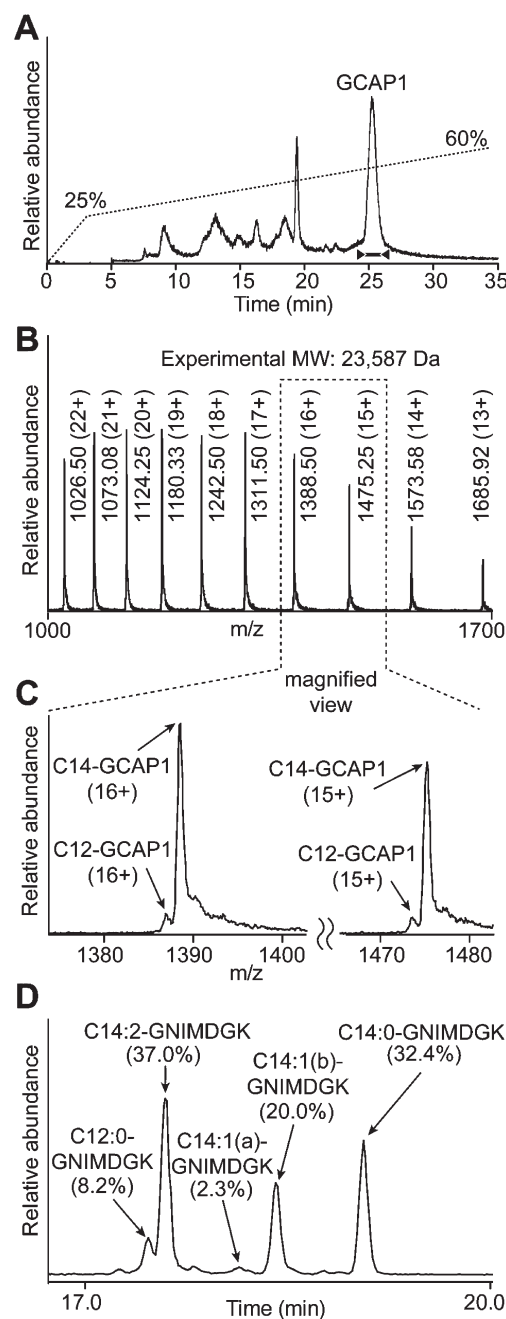

Figure 2. LC/MS analysis of N-terminally acylated GCAP1 from bovine retina. (A) LC/MS chromatogram of the GCAP1 preparation. A horizontal bar below the base peak in (A) marks the time interval over which the MS spectrum (B) was averaged. MS spectral peaks annotated with m/z values and charges (inside brackets) represent consecutive charged states of an individual protein. (B, top) The protein's MW (23 587 Da) computed from m/z values of its charged states (see Experimental Procedures) closely matches the theoretical MW of myristoylated GCAP1 (23 589 Da) indicating that GCAP1 with a 14-carbon saturated or unsaturated acyl group is the predominant form in the retina. A magnified view of individual charged states (C) reveals that lauroylated GCAP1 (computed and theoretical MWs match exactly at 23 561 Da) also is present at 8.5 ± 0.3% of total GCAP1. (D) LC/MS chromatogram of a tryptic digest of GCAP1 from bovine retina showing acylated N-terminal peptides. The relative abundance of each peptide, calculated from the area under the appropriate peak, is given in brackets. The MS/MS spectra are presented in Figure S-1 of the Supporting Information.

insert vial and directly injected into the LC/MS instrument. MS and MS/MS analyses revealed that the N-terminal GCAP1 peptide (GNIMDGK) was modified with five different fatty acids: C14:0, C14:1 (a), C14:1 (b), C14:2, and C12:0 (Figure 2D, Figure S-1). Surprisingly, two different chromatographic peaks contained C14:1-GNIMDGK as revealed by MS and MS/MS spectra. This suggested that GNIMDGK was present as two isomers of C14:1 fatty acid that we annotated as (a) and (b). The acyl moiety of the abundant C14:1(b)-GNIMDGK is most likely the *cis*-Δ5-C14:1 isomer previously reported as one of the N-terminal acyl moieties of retinal proteins.[4,5] C14:1(a)-GNIMDGK was barely detectable so we did not attempt to determine the position of the double bond in its acyl moiety. The relative abundance of acyl-GNIMDGK peptides was 37.0% (C14:2), 32.4% (C14:0), 20.0% (C14:1 (b)), 8.3% (C12:0), and 2.3% (C14:1 (a)) as quantified from areas under the peaks of the selected ion chromatogram. Importantly, other modifications were not detected. Moreover, because the signal-to-noise ratio in our MS analysis was above 30 even for the sparse C12:0-GNIMDGK, it is unlikely that any other acyl-GCAP1 variants were present in physiologically relevant quantities. Both intact protein and peptide analyses consistently showed that C12:0-GCAP1 constitutes only ∼8.5% of the total acylated GCAP1 while the remaining 91.5% is acylated with various 14-carbon fatty acids.

Ratios of C14:2-CoA and C14:1-CoA to C14:0-CoA Are Higher in the Retina Than in the Brain. The reason why heterogeneous N-acylation is restricted to retinal proteins has yet to be clarified. One possible explanation is that C12:0-, C14:1-, and C14:2-CoA, the unusual NMT substrates, are enriched in the retina relative to C14:0-CoA. To test this hypothesis, we performed comparative LC/MS analyses of acyl-CoAs purified from bovine retina and brain. We selected the brain as a reference because it was demonstrated that the C-subunit of PKA from bovine brain does not undergo heterogeneous N-acylation, whereas the same enzyme from bovine retina does.[7] The acyl-CoAs were purified from both tissues following exactly the same procedure to ensure their accurate quantification and then analyzed by LC/MS (see Experimental Procedures). The selected ion chromatograms of acyl-CoAs purified from retina (Figure 3A) and brain (Figure 3B) displayed well-separated medium- and long-chain acyl-CoAs. Short chain acyl-CoAs and the free coenzyme A also were detected (not shown). Peak identities were assigned based on m/z values, and in most cases, were further confirmed by MS/MS analysis (Figures S-2 and S-3). Upon examination of the spectral peaks, it was immediately apparent that the acyl-CoA profiles of the brain and the retina differed substantially. Importantly, close inspection of the spectral peaks corresponding to 14-carbon acyl-CoAs (Figure 3C,D) revealed that the ratios of C14:2- and C14:1-CoA to C14:0-CoA were elevated in the retina relative to the brain. Interestingly, two isomers of C14:1-CoA were present as determined from identical m/z values and similar MS/MS spectra. This observation is consistent with our finding that GCAP1 can be modified with two different C14:1 fatty acids. The more abundant C14:1(b)-CoA is most likely the *cis*-Δ5-C14:1-CoA previously reported to serve as a substrate for the N-acylation of retinal proteins. We did not attempt to establish the position of the double bond in the C14:1(a)-CoA. To compare the acyl-CoA profiles of both tissues, areas under the chromatographic peaks were measured and the obtained values were normalized to the total acyl-CoA signal (Figure 3E). On the basis of this analysis, the ratios of

14-carbon unsaturated NMT substrates C14:2-, C14:1(a)-, and C14:1(b)-CoA to the total acyl-CoA were respectively 7.0-, 3.8-, and 3.7-fold higher in the retina than in the brain. The ratio of myristoyl-CoA (C14:0-CoA), the typical NMT substrate, to total acyl-CoA was only slightly higher (1.4-fold) in the retina than in the brain, and this difference was not statistically significant according to Student t test. The ratio of C12:0-CoA to total acyl-CoA was nearly the same in both tissues as well. Remarkably, the ratios of both C18:2- and C16:2-CoA to total acyl-CoA were much higher in the retina than in the brain, 6.7- and 19.0-fold, respectively. Notably, C18:2- and C16:2-CoA were previously shown to undergo conversion to C14:2-CoA through β-oxidation (Figure 4).[20] Similarly, C16:1 and C18:1 were suggested to be putative precursors of C14:1-CoA. The ratio of C16:1 to total acyl-CoA was only slightly higher in the retina than in the brain, whereas the ratio of C18:1 to total acyl-CoA was higher in the brain. This is not surprising as C16:1-CoA and C18:1-CoA can be synthesized *de novo* in the cytoplasm (Figure 4). Interestingly, the ratio of C18:3-CoA, an intermediate in the synthesis of long polyunsaturated fatty acids, to total acyl-CoA was also highly elevated in the retina. However, we were not able to distinguish if this peak represents C18:3-n6, C18:3-n3, or a mixture of both. Normalization of the data to the C14:0-CoA signal, instead of the total-CoA signal, yielded similar results (Figure 3F). Ratios of C14:2-, C14:1(a)-, and C14:1(b)-CoA, unusual substrates for N-acylation of proteins, to C14:0-CoA were elevated in the retina relative to the brain by 4.6-, 2.8-, and 2.7-fold, respectively. Thus, these differences could contribute to the heterogeneous N-acylation of retinal proteins. Because some C14:2- and C14:1-CoAs are also detectable in the brain and the ratios of C12:0-CoA/C14:0-CoA are similar in both retina and brain, additional factors like, e.g., intracellular distribution of N-acylation substrates need to be taken into account to fully explain the retinal specificity of heterogeneous N-acylation.

***In Vitro* Production of Acyl-GCAP1 Variants.** Our next goal was to determine how various acyl moieties affect the activity of GCAP1. This objective required highly purified acyl-GCAP1 variants. We initially considered purifying GCAP1 from native sources and then separating its acylated variants by HPLC. However, this approach was not feasible for the following reasons. First, our assays required ∼800 μg of each acyl-GCAP1 variant, and we were able to obtain only 100−200 μg of total GCAP1 from 120 retinas. Second, adequate HPLC separation of protein variants that differ solely by their acyl moieties is not readily feasible; only partial success has been reported thus far.[10] Because of these limitations, we decided to generate acyl-GCAP1 variants by adapting our method of *in vitro* protein myristoylation[29] to accommodate fatty acids other than myristoyl. The sequence of recombinant GCAP1 that served as the acylation substrate contained an N-terminal His-tag followed by the TEV protease recognition site (Figure 5A,B). The Gly residue, an obligatory fatty acid acceptor in NMT-catalyzed reactions, was exposed by TEV cleavage. The amounts of reactants in the acylation reaction and their mixing order were crucial. The molar ratio of the enzyme (NMT), substrate (acyl-CoA), and target protein (GCAP1) was 4:2:1 in the initial reaction mixture. The acyl-CoA was added to the NMT, and a secondary complex[30] was allowed to form prior to addition of the target protein. Sequestration of the substrate (acyl-CoA) in the binding pocket of NMT prevents it from clinging to hydrophobic surfaces of the target protein, thus increasing its availability for the acylation reaction and facilitating its separation from the protein product. A substantial
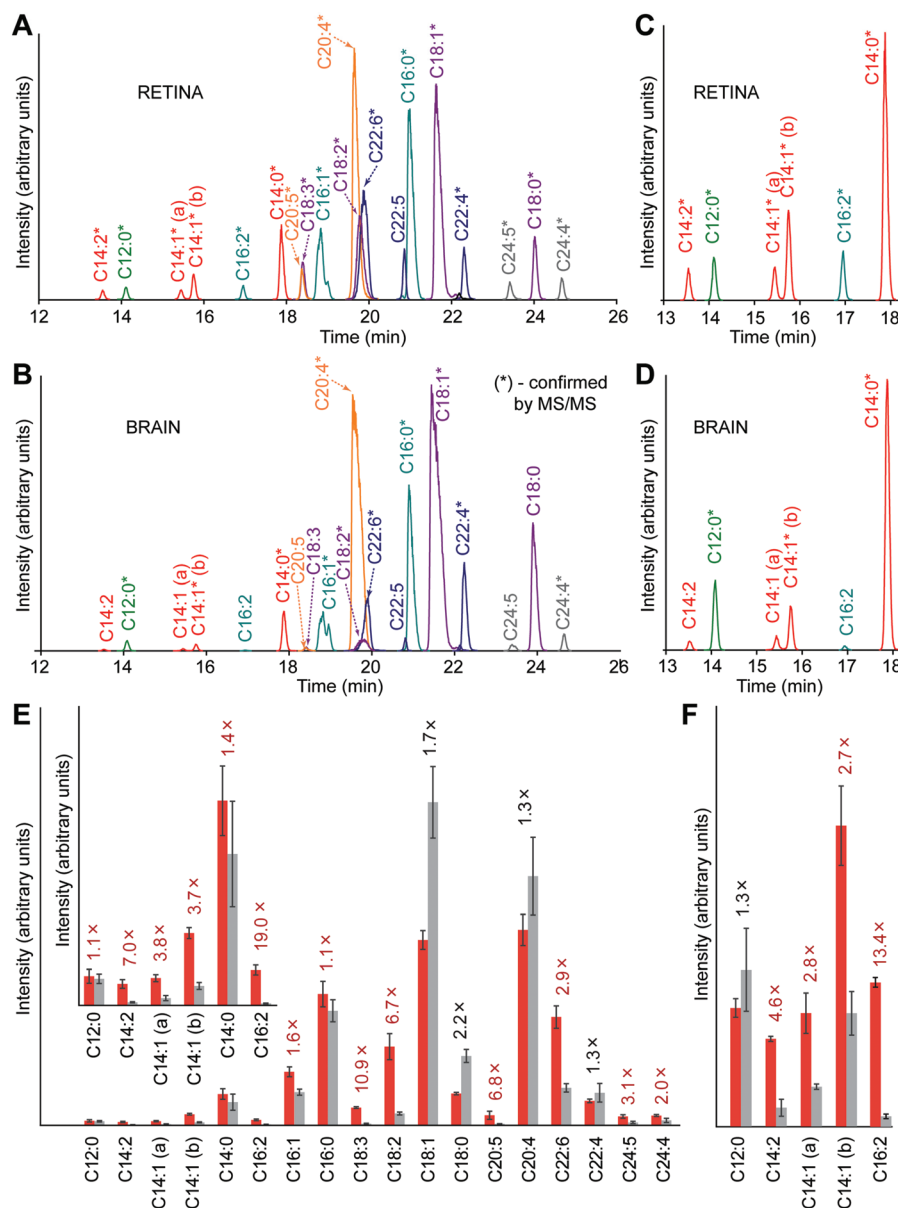
Figure 3. LC/MS analysis of acyl-CoAs from bovine retina and brain. Representative selected ion chromatograms of acyl-CoAs from bovine retina (A, C) and brain (cerebral region) (B, D) with (C and D) presenting an expanded view of acyl-CoAs that serve as substrates for N-terminal protein acylation. The same color is used to indicate peaks representing acyl-CoAs with the same number of carbons in the acyl moiety. Identities of peaks marked with an asterisk were confirmed by MS/MS analyses with examples presented in Figure S-3 of the Supporting Information. Some low-abundance species were omitted for clarity. Areas under the chromatographic peaks were measured for at least three experimental replicates, and the mean values, normalized to either the total acyl-CoA or C14-CoA signal, were plotted in (E) and (F), respectively. The red and gray bars represent retinal and cerebral samples, respectively, and the numbers above indicate the fold differences between them. These numbers are colored red or black for the retina- or brain-enriched acyl-CoAs, respectively. Vertical lines represent standard deviations of the means. The inset in (E) depicts a magnified view of the plot. Attributable to differences in ionization efficiency, only the same acyl-CoA species can be quantitatively compared. The C16:1-CoA peak had at least one shoulder, suggesting isomers that were quantified together. These data demonstrate significant differences in acyl-CoA profiles of bovine retina and brain. Importantly the ratios of unsaturated NMT substrates (C14:1-CoA and C14:2-CoA) to C14:0-CoA are higher in the retina than in the brain. This is proposed to be a major cause of retina-specific heterogeneous N-acylation.

excess of enzyme over the acyl-CoA was used to compensate for the inaccuracy of substrate concentration measurements and potential partial inactivation of the enzyme. The above method was efficient in generating myristoylated proteins. However, attempts to acylate GCAP1 with other fatty acids resulted in a mixture containing 60% of the desired acyl-GCAP1 and a 40% of contaminating myristoyl-GCAP1 (not shown). The source of this contamination became evident after additional experiments

revealed that 10−15% of NMT purified from bacteria was complexed with C14:0-CoA (not shown). To release this pre-bound C14:0-CoA, the NMT preparation was incubated with a substrate octapeptide (GARASVLS-NH$_2$)[26] that after acyl transfer was removed by size-exclusion chromatography. NMT pretreated in this manner was then successfully used to generate C12:0-GCAP1 and C15:0-GCAP1 in addition to C14:0-GCAP1 (Figure 6A−C). Moreover, we observed that a longer incubation
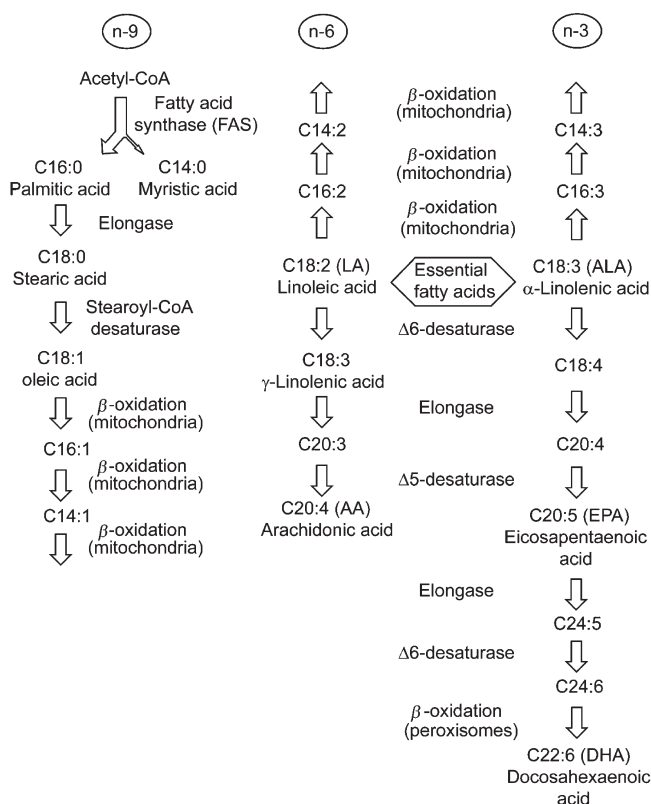
Figure 4. Selected pathways of fatty acid metabolism. This figure is modified from ref 52.

time and higher temperature were required to acylate GCAP1 with C12:0-CoA than with C14:0-CoA, indicating that C12:0-CoA is an inferior NMT substrate compared to C14-CoA. We also tried to acylate GCAP1 with C8:0-, C10:0-, and C16:0-CoA substrates but could only acylate a small fraction of the target protein. Extending incubation time and elevating temperature did not result in substantial improvement. Taken together, these results confirm that NMT is highly selective for 14-carbon acyl-CoAs. This rigorous specificity is the likely reason why native GCAP1 is acylated predominantly with 14-carbon fatty acids with a small admixture of C12:0.

GCAPs with N-Terminal Acyl Moieties of Various Lengths Have Comparable Functionality. An objective of our experiments was to determine whether slight differences in the length of the acyl moiety can distinctly affect GCAP's Ca^{2+} sensitivity and its ability to activate GC1. So we compared non-acylated GCAP1, C12-GCAP1, C14-GCAP1, and C15-GCAP1. The GC1-stimulatory activity of these acylated GCAP1 variants was tested in cGMP production radioassays. Measurements of concentration-dependent responses of GC1 to these variants (Figure 7A) allowed us to determine maximal cGMP production rates and half-maximal effective acyl-GCAP1 concentrations (EC_{50}) (Figure 7A, bottom panel). These results clearly demonstrate that acyl-GCAPs increase cGMP production about 3-fold relative to the non-acylated protein. Differences between the acyl-GCAP1 variants were small. The maximal cGMP production rate obtained for GC1 in the presence of C12-GCAP1 (8.81 ± 0.85 nmol/min/million cells) seemed slightly higher than those obtained in the presence of C14-GCAP1 (8.12 ± 0.21 nmol/min/million cells) and C15-GCAP1 (8.02 ±
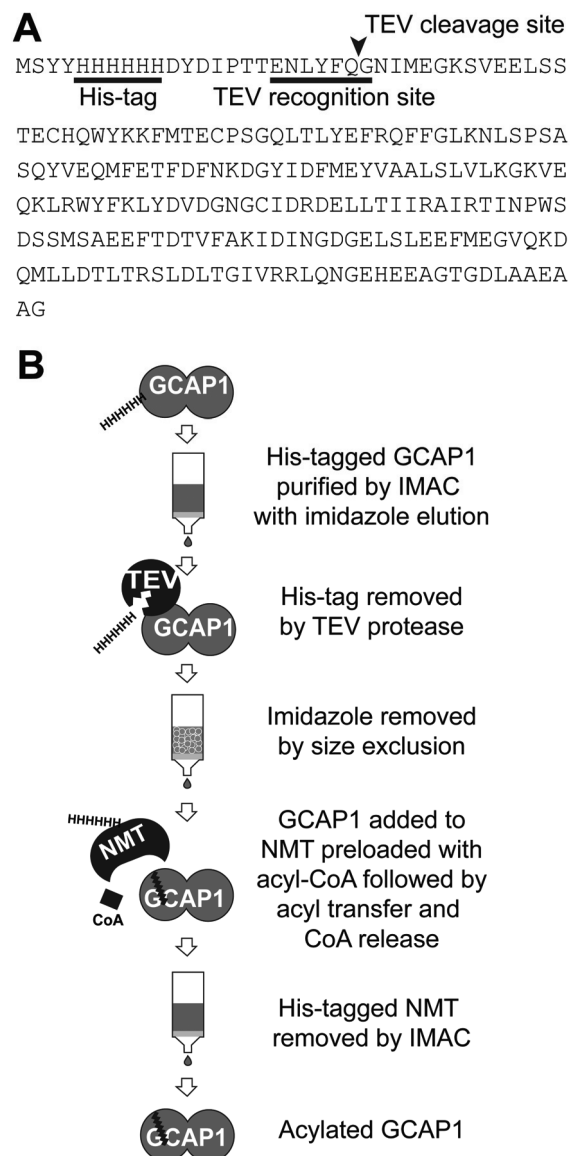

Figure 5. Expression and *in vitro* N-acylation of mouse GCAP1. (A) Sequence of recombinant mouse GCAP1 with the N-terminal His-tag preceding the TEV protease recognition site. TEV cleavage exposes Gly, an acyl acceptor, as the N-terminal residue. This design allows efficient purification and *in vitro* N-acylation of GCAP1, presented stepwise in (B).

0.73 nmol/min/million cells), but the differences were not statistically significant. EC_{50} values obtained for C12-, C14-, and C15-GCAP1 were 4.23 ± 0.04, 5.50 ± 0.54, and 7.03 ± 0.14 μM, respectively. Thus, only a slight increase in EC_{50} of acyl-GCAP1 with the increased length of the acyl moiety was observed. We also assayed the Ca^{2+} sensitivity of non-acylated GCAP1 and its acylated variants and determined the half-maximal effective concentrations of free Ca^{2+} (EC_{50}) (Figure 7B). Our results demonstrate that C12-, C14-, and C15-GCAP1 exhibited similar Ca^{2+} sensitivities in contrast to non-acylated GCAP1 that was less sensitive to Ca^{2+}. The EC_{50} values for free Ca^{2+} were 886 ± 109, 466 ± 80, 359 ± 25, and 360 ± 49 nM for non-acylated, C12-, C14-, and C15-GCAP1, respectively.
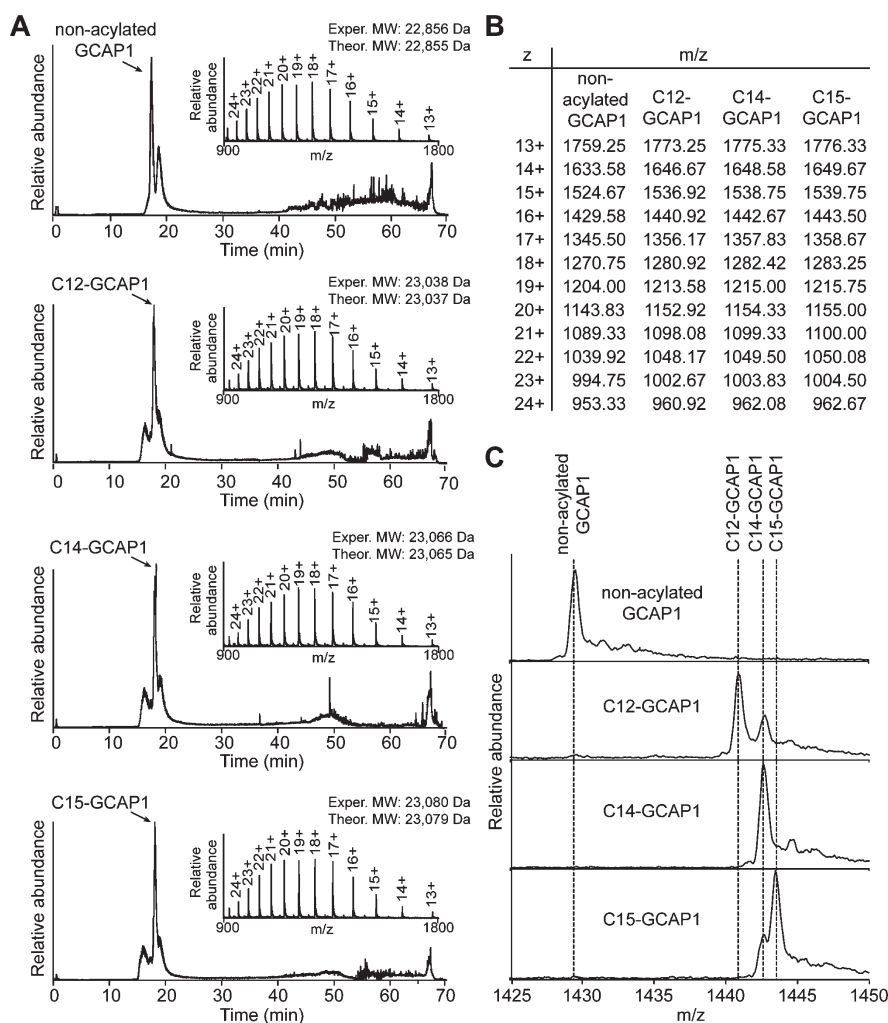
Figure 6. LC/MS analysis of GCAPs N-terminally acylated *in vitro*. (A) LC/MS chromatograms of non-acylated GCAP1 as well as GCAP1 modified with N-terminal lauroyl (C12), myristoyl (C14), and pentadecanoyl (C15) moieties. MS spectra (insets) were recorded for the highest peak in each chromatogram. Multiple peaks of these MS spectra correspond to consecutive charged states of an intact protein. Experimental and theoretical MWs for the corresponding GCAP1 variants are shown above the MS spectra. Theoretical MWs were computed from a protein's sequence plus the MW of its appropriate acyl moiety, and experimental MWs were calculated from m/z values of the protein's charged states (B) as described in the Experimental Procedures section. Similarities between experimental and theoretical MWs confirm that acylation was successful. A small peak or a shoulder that follows the highest peak in each chromatogram was identified as a dimer of the sample-specific GCAP1 variant and peaks preceding GCAPs represent contaminants with heterogeneous m/z values. (C) Expanded MS spectra of the 16+ charged state with vertical lines denoting positions of different GCAP1 variants. This data representation reveals that C14-GCAP1 contaminates C12-GCAP1 and C15-GCAP1 preparations in amounts of ~10% and ~25%, respectively, confirming that the purity of these preparations is adequate for the experiments described.

■ DISCUSSION

Emergence of the heterogeneous N-acylation expanded retinal proteome. Because of heterogeneous N-acylation, each modified protein is present in four variants that differ in the hydrophobicity and the rigidity of their N-acyl moieties. To examine the overall effect of heterogeneous N-acylation on retinal physiology does not seem feasible because there are yet no means to selectively ablate N-acylation with C14:2, C14:1, and C12:0 fatty acids *in vivo*. However, effects of heterogeneous N-acylation on the function of individual proteins can be examined. Here we have for the first time investigated how acyl moieties of different lengths (C12:0, C14:0, and C15:0) and thus different hydrophobicity affect the activity of GCAP1. Our results demonstrated that all acyl-GCAP1 variants (1) were fully functional, in contrast to non-acylated GCAP1, (2) stimulated

GC1 to a similar maximal activity, and (3) evidenced similar Ca^{2+} sensitivity. Surprisingly, the EC_{50} of C12-GCAP1 was slightly lower than that of C14-GCAP1, and the EC_{50} of C14-GCAP1 was slightly lower than of C15-GCAP1. Because each of the acyl-GCAP1 variants had to be individually acylated and purified, these small differences could result from sample handling. Alternatively, it is possible that the C12-GCAP1 can transition into an active state more rapidly than GCAPs with longer acyl moieties. Structural studies of GCAP1 that could permit further clarification of this result are ongoing. Moreover, the mechanism through which acyl moiety enhances GCAP1's activity remains elusive. Currently, the prevailing view is that the acyl moiety remains buried in the hydrophobic cleft of GCAP1's N-terminal lobe, independent of Ca^{2+} concentration.[17,18] Permanently sequestered within GCAP1's structure the acyl moiety
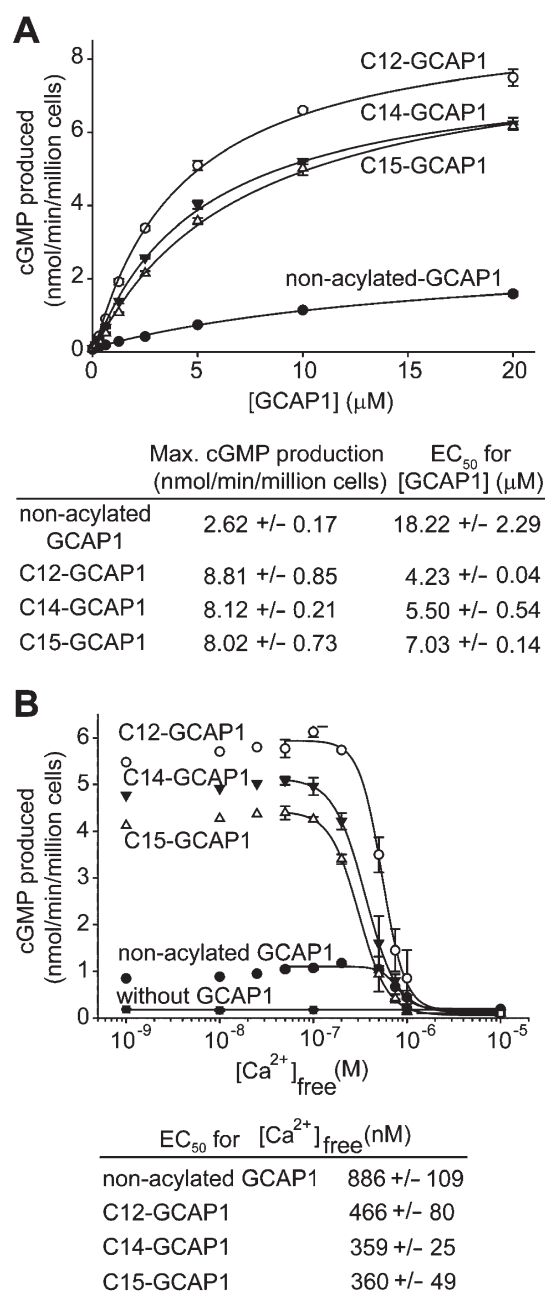
Figure 7. Properties of GCAPs with different N-terminal acyl moieties. (A) Concentration-dependent response of GC to GCAPs with different N-terminal acyl moieties as well as to non-acylated GCAP1 and (B) Ca^{2+} sensitivity of these GCAPs determined by cGMP production radioassays with sonicates of HEK-293 cells overexpressing GC. Table (A, bottom panel) shows maximal cGMP production rates as well as half-maximal effective concentrations (EC_{50}) for GCAP1, which were calculated as parameters of a hyperbolic fitting function. Average values from two experiments with triplicate samples are shown. (B, bottom panel) shows half-maximal effective concentrations of free Ca^{2+} calculated using a four-parameter logistic function fitted to the data points within a 50 nmol to 5 μM Ca^{2+} concentration range. Averaged values from three experiments with triplicate samples are listed. In the Ca^{2+}-sensitivity experiments, GCAP concentrations were 6.5 μM (experiment 1) and 4 μM (experiments 2 and 3). Results indicate that all acylated GCAPs are effective GC activators and respond to changes in Ca^{2+} concentration in a similar manner. This differs from non-acylated GCAP, which is a weaker activator regulated within a higher Ca^{2+} range.

could participate in stabilizing the active conformation upon dissociation of Ca^{2+}. However, because majority of experiments supporting this model were carried out in the absence of lipids and GC, alternative hypotheses proposing that the acyl moiety might enhance the interaction of GCAP1 with membranes or with GC should also be considered.

Long-chain acyl dehydrogenase deficiency in a subset of retinal cells is a possible cause of retinal heterogeneous N-acylation. Previously, DeMar et al. suggested that β-oxidation could be the major source of C14:2- and C14:1-CoA that serve as substrates for the heterogeneous N-acylation of retinal proteins[20] (Figure 4). However, the question remained: Why is heterogeneous N-acylation restricted to the retina? Our results demonstrate that the ratios of C14:2- and C14:1-CoA to C14:0-CoA were substantially elevated in the retina compared to the brain. Moreover, the potential C14:2-CoA precursors, namely C16:2-, C18:2-, and C18:3-CoA, were also elevated relative to total acyl-CoA in the retina. Thus, we investigated whether there is anything unusual about retinal fatty acid β-oxidation that could account for these differences. Recently, Atsuzawa et al. demonstrated that retinal levels of β-oxidation enzymes were much lower than their liver levels,[31] which suggests that retinal β-oxidation is greatly reduced. What we found especially intriguing was a low expression level, relative to other β-oxidation enzymes, of the long-chain acyl dehydrogenase (LCAD). The effect of LCAD deficiency on fatty acid metabolism was previously studied in $Lcad^{-/-}$ mice.[32] Strikingly, these animals had highly elevated levels of C14:2 and C14:1 fatty acids in both the serum and liver as well as corresponding carnitine esters in their blood and skeletal muscle. C12:0 fatty acid was elevated in the liver but not in the serum, and a statistically significant increase of C18:1 and C18:2 in the serum was also observed. Thus, C14:2- and C14:1-CoA, substrates for N-acylation that we found elevated in the retina, are also highly elevated in $Lcad^{-/-}$ mice. Together with the low level of retinal LCAD, these data suggest that a subset(s) of retinal cells could be deficient in this enzyme (or enzyme with similar activity) and consequently generate increased amounts of C14:2-, C14:1-, and C12:0-CoAs.

LCAD is one of several acyl dehydrogenases that catalyze the first reaction of mitochondrial β-oxidation. The others are medium-chain acyl dehydrogenase (MCAD), very-long-chain acyl dehydrogenase (VLCAD), and acyl-CoA dehydrogenase 9 (ACAD-9).[33−35] Various acyl dehydrogenases have different, often overlapping, substrate specificities. Their substrates differ by chain length as well as the number and position of double bonds.[33] Thus, expression levels of acyl dehydrogenases directly affect the acyl-CoA pool of the cell.

An intriguing question is, which cell type(s) are responsible for the production of the unusually high amounts of C14:2-, C14:1-, and 12:0-CoAs in the retina? Photoreceptors seem to be the primary candidate as the photoreceptor-specific GCAP1 is heterogeneously acylated. Moreover, immunocytochemical experiments reported by Tyni et al. suggest that the mitochondrial trifunctional protein, which contains three out of four β-oxidation enzymatic activities, is present in photoreceptor inner segments.[36] This implies that these cells could carry out β-oxidation. Furthermore, medium-chain acyl dehydrogenase MCAD was not detected in photoreceptors, suggesting that β-oxidation in these cells is partial. Expression of LCAD has not been tested. The RPE cells also appear a likely candidate as these cells export fatty acids to photoreceptor cells and express enzymes for fatty acid β-oxidation.[36,37] However, our preliminary

results (Western blot analyses) revealed that RPE cells express LCAD, ACAD9, and VLCAD (Figure S-4), implying that these cells are unlikely to produce unusually high amounts of C14:2- and C14:1-CoA. In the future, localization of β-oxidation enzymes at cellular resolution and acyl-CoAs with subcellular resolution should permit identification of the cell type(s) that generate increased amounts of C14:2-, C14:1-, and C12:0-CoA as well as those cells in which heterogeneous N-acylation occurs.

Our experiments demonstrate that the ratios of C14:2- and C14:1-CoA to C14:0-CoA were 4.6 and 2.7 times higher in the retina than in the brain. These differences do not seem sufficient to explain the retinal specificity of heterogeneous N-acylation. However, if heterogeneous N-acylation is restricted to photoreceptors, then the ratios of C14:2- and C14:1-CoA to C14:0-CoA in these cells would be much greater. We do not have a clear explanation of why C12:0-proteins are detectable exclusively in the retina despite similar ratios of C12:0-CoA/C14:0-CoA in the retina and in the brain. Surprisingly, the C12:0-CoA results were also peculiar in the *Lcad*^{−/−} mouse study as this compound was highly elevated in the liver but not in the serum.[32]

The observation that the ratios of various N-acyl moieties of distinct proteins vary[20] seems to be inconsistent with unusual acyl-CoA pool being a major cause of heterogeneous N-acylation. This apparent discrepancy could be attributed to the following: (i) The efficiency of acyl-protein release from the membrane depends on the type of protein itself, the character of the acyl moiety, and the solvent used. Thus, differences in purification methods could have resulted in observed different ratios of acyl moieties. (ii) Various NMT-acyl-CoA complexes could differ in their affinities for different polypeptides. The observation that the C14:0-CoA analogue forms part of the substrate binding site in the crystal structure of NMT[38] supports this hypothesis. (iii) If heterogeneous N-acylation is more pronounced in a particular subset of retinal cells, e.g. photoreceptors, a protein expressed throughout the retina should have higher C14:0 content than a protein that is photoreceptor-specific. A possible example could be that, whereas 57% of ubiquitously expressed C-subunit of PKA purified from the retina contains C14:0, only 32.4% of photoreceptor-specific GCAP1 is modified with this fatty acid (this report and ref 7).

DeMar et al. have suggested that peroxisomal β-oxidation is most likely to be responsible for production of C14:2- and C14:1-CoA.[20] Peculiarly, St. Jules et al. reported the presence of peroxisomes in frog Müller cells and cones but were not certain about the presence of these organelles in rod photoreceptors.[39] Theoretically, C14:2- and C14:1-CoA could be produced in peroxisomes of cones and Müller cells and then be transported to rod photoreceptors. However, compared with mitochondria, peroxisomes seem to be a minor site for β-oxidation.[40]

In short, a possible scenario that explains why heterogeneous N-acylation is restricted to retinal proteins is the following: The availability of C14:0-CoA to NMT seems to be good in all cell types because of its *de novo* synthesis via cytoplasmic fatty acid synthase (FAS) (Figure 4).[41,42] C14:2-, C14:1-, and C12:0-CoAs are generated in the mitochondria as intermediate products of β-oxidation that typically do not accumulate and are not exported to the cytoplasm in quantities that could result in detectable heterogeneous N-acylation. However, our data in conjunction with studies of LCAD[31,32] led us to formulate a hypothesis that limited β-oxidation in the retina, at the level of acyl-CoA dehydrogenase, results in mitochondrial accumulation of these acyl-CoAs and their export to the cytoplasm (the site of protein

N-acylation). Import of acyl-CoA from mitochondria is possible via the carnitine shuttle.[43−45] Limited β-oxidation in the retina could have additional consequences, e.g., accumulation of precursors for synthesis of long unsaturated fatty acids, which are important for retina's function.[37,46−48]

In summary, we found that 14-carbon unsaturated fatty acids are the most common N-acyl moieties of GCAP1. Moreover, we developed a new method for *in vitro* protein N-acylation. Acylated GCAP1s were more active and more sensitive to Ca^{2+} than non-acylated GCAP1, while the length of the acyl moiety seemed to have only a minor effect on acyl-GCAP1 function. Extensive quantitative analysis of acyl-CoAs from bovine retina and brain revealed substantial differences in the acyl-CoA profiles between these two tissues. The ratios of uncommon substrates for N-acylation, C14:1- and C14:2-CoA, to C14:0-CoA were elevated in the retina relative to the brain. Also, the ratios of C18:3- and C22:6-CoA to total acyl-CoA were higher in the retina then in the brain. C18:3-CoA is the precursor for synthesis of long polyunsaturated fatty acids, and C22:6 is crucial for photoreceptor function. These results show that retina-specific lipid metabolism is employed to generate substrates for retina-specific protein modifications that expand the retinal proteome. Thus, this work increases understanding of basic biochemical processes in the animal eye and sets a framework for future experimentation.

■ ASSOCIATED CONTENT

S **Supporting Information.** Four additional figures presenting MS/MS spectra of acylated N-terminal peptides from GCAP1, MS/MS fragmentation pattern of C14-CoA, MS/MS spectra of various acyl-CoAs, and immunoblots of acyl dehydrogenases from RPE cells, liver, and brain. This material is available free of charge via the Internet at http://pubs.acs.org.

■ AUTHOR INFORMATION

Corresponding Author
*E-mail: kxp65@cwru.edu. Phone: (216) 368-4631. Fax: (216) 368-1300.

■ DEDICATION

We dedicate this work to our former postdoctoral fellow Dr. Wojciech Gorczyca, who discovered GCAPs. Dr. Gorczyca, who passed away September 24, 2010, made outstanding contributions to this field. Along with other laboratory members, we deeply feel his loss.

■ ABBREVIATIONS

ACAD-9, acyl-CoA dehydrogenase 9; CACT, carnitine-acylcarnitine translocase; CoA, coenzyme A; CPT, carnitine palmitoyl transferase; DHA, docosahexaenoic acid; GC, guanylate cyclase; GCAP1, guanylate cyclase-activating protein 1; LCAD, long-chain acyl dehydrogenase; LC/MS, liquid chromatography coupled mass spectrometry; MCAD, medium-chain acyl dehydrogenase; MS, mass spectrometry (spectrometer); MS/MS, tandem mass spectrometry; MW, molecular weight; m/z, mass to charge ratio; NMT1, N-myristoyltransferase 1; VLCAD, very-long-chain acyl dehydrogenase.

■ REFERENCES

(1) Arnesen, T., Van Damme, P., Polevoda, B., Helsens, K., Evjenth, R., Colaert, N., Varhaug, J. E., Vandekerckhove, J., Lillehaug, J. R., Sherman, F., and Gevaert, K. (2009) Proteomics analyses reveal the evolutionary conservation and divergence of N-terminal acetyltransferases from yeast and humans. *Proc. Natl. Acad. Sci. U.S.A.* 106, 8157–8162.

(2) Hwang, C. S., Shemorry, A., and Varshavsky, A. (2010) N-terminal acetylation of cellular proteins creates specific degradation signals. *Science* 327, 973–977.

(3) Wright, M. H., Heal, W. P., Mann, D. J., and Tate, E. W. (2009) Protein myristoylation in health and disease. *J. Chem. Biol.* 3, 19–35.

(4) Kokame, K., Fukada, Y., Yoshizawa, T., Takao, T., and Shimonishi, Y. (1992) Lipid modification at the N terminus of photoreceptor G-protein alpha-subunit. *Nature* 359, 749–752.

(5) Dizhoor, A. M., Ericsson, L. H., Johnson, R. S., Kumar, S., Olshevskaya, E., Zozulya, S., Neubert, T. A., Stryer, L., Hurley, J. B., and Walsh, K. A. (1992) The NH2 terminus of retinal recoverin is acylated by a small family of fatty acids. *J. Biol. Chem.* 267, 16033–16036.

(6) Neubert, T. A., Johnson, R. S., Hurley, J. B., and Walsh, K. A. (1992) The rod transducin alpha subunit amino terminus is heterogeneously fatty acylated. *J. Biol. Chem.* 267, 18274–18277.

(7) Johnson, R. S., Ohguro, H., Palczewski, K., Hurley, J. B., Walsh, K. A., and Neubert, T. A. (1994) Heterogeneous N-acylation is a tissue- and species-specific posttranslational modification. *J. Biol. Chem.* 269, 21067–21071.

(8) Palczewski, K., Subbaraya, I., Gorczyca, W. A., Helekar, B. S., Ruiz, C. C., Ohguro, H., Huang, J., Zhao, X., Crabb, J. W., and Johnson, R. S. et al. (1994) Molecular cloning and characterization of retinal photoreceptor guanylyl cyclase-activating protein. *Neuron* 13, 395–404.

(9) DeMar, J. C., Jr., and Anderson, R. E. (1997) Identification and quantitation of the fatty acids composing the CoA ester pool of bovine retina, heart, and liver. *J. Biol. Chem.* 272, 31362–31368.

(10) Sanada, K., Kokame, K., Yoshizawa, T., Takao, T., Shimonishi, Y., and Fukada, Y. (1995) Role of heterogeneous N-terminal acylation of recoverin in rhodopsin phosphorylation. *J. Biol. Chem.* 270, 15459–15462.

(11) Polans, A., Baehr, W., and Palczewski, K. (1996) Turned on by Ca2+! The physiology and pathology of Ca(2+)-binding proteins in the retina. *Trends Neurosci.* 19, 547–554.

(12) Subbaraya, I., Ruiz, C. C., Helekar, B. S., Zhao, X., Gorczyca, W. A., Pettenati, M. J., Rao, P. N., Palczewski, K., and Baehr, W. (1994) Molecular characterization of human and mouse photoreceptor guanylate cyclase-activating protein (GCAP) and chromosomal localization of the human gene. *J. Biol. Chem.* 269, 31080–31089.

(13) Gorczyca, W. A., Polans, A. S., Surgucheva, I. G., Subbaraya, I., Baehr, W., and Palczewski, K. (1995) Guanylyl cyclase activating protein. A calcium-sensitive regulator of phototransduction. *J. Biol. Chem.* 270, 22029–22036.

(14) Dizhoor, A. M., Olshevskaya, E. V., Henzel, W. J., Wong, S. C., Stults, J. T., Ankoudinova, I., and Hurley, J. B. (1995) Cloning, sequencing, and expression of a 24-kDa Ca(2+)-binding protein activating photoreceptor guanylyl cyclase. *J. Biol. Chem.* 270, 25200–25206.

(15) Venkatesan, J. K., Natarajan, S., Schwarz, K., Mayer, S. I., Alpadi, K., Magupalli, V. G., Sung, C. H., and Schmitz, F. (2010) Nicotinamide adenine dinucleotide-dependent binding of the neuronal Ca2+ sensor protein GCAP2 to photoreceptor synaptic ribbons. *J. Neurosci.* 30, 6559–6576.

(16) Payne, A. M., Downes, S. M., Bessant, D. A., Taylor, R., Holder, G. E., Warren, M. J., Bird, A. C., and Bhattacharya, S. S. (1998) A mutation in guanylate cyclase activator 1A (GUCA1A) in an autosomal dominant cone dystrophy pedigree mapping to a new locus on chromosome 6p21.1. *Hum. Mol. Genet.* 7, 273–277.

(17) Stephen, R., Bereta, G., Golczak, M., Palczewski, K., and Sousa, M. C. (2007) Stabilizing function for myristoyl group revealed by the crystal structure of a neuronal calcium sensor, guanylate cyclase-activating protein 1. *Structure* 15, 1392–1402.

(18) Lim, S., Peshenko, I., Dizhoor, A., and Ames, J. B. (2009) Effects of Ca2+, Mg2+, and myristoylation on guanylyl cyclase activating protein 1 structure and stability. *Biochemistry* 48, 850–862.

(19) Gorczyca, W. A. (2000) Use of nucleoside alpha-phosphorothioates in studies of photoreceptor guanylyl cyclase: purification of guanylyl cyclase activating proteins. *Methods Enzymol.* 315, 689–707.

(20) DeMar, J. C., Jr., Rundle, D. R., Wensel, T. G., and Anderson, R. E. (1999) Heterogeneous N-terminal acylation of retinal proteins. *Prog. Lipid Res.* 38, 49–90.

(21) Rundle, D. R., Rajala, R. V., Alvarez, R. A., and Anderson, R. E. (2004) Myristoyl-CoA:protein N-myristoyltransferases: isoform identification and gene expression in retina. *Mol. Vis.* 10, 177–185.

(22) Liang, X., Nazarian, A., Erdjument-Bromage, H., Bornmann, W., Tempst, P., and Resh, M. D. (2001) Heterogeneous fatty acylation of Src family kinases with polyunsaturated fatty acids regulates raft localization and signal transduction. *J. Biol. Chem.* 276, 30987–30994.

(23) Kishore, N. S., Wood, D. C., Mehta, P. P., Wade, A. C., Lu, T., Gokel, G. W., and Gordon, J. I. (1993) Comparison of the acyl chain specificities of human myristoyl-CoA synthetase and human myristoyl-CoA:protein N-myristoyltransferase. *J. Biol. Chem.* 268, 4889–4902.

(24) Minkler, P. E., Kerner, J., Ingalls, S. T., and Hoppel, C. L. (2008) Novel isolation procedure for short-, medium-, and long-chain acyl-coenzyme A esters from tissue. *Anal. Biochem.* 376, 275–276.

(25) Wan, J., Roth, A. F., Bailey, A. O., and Davis, N. G. (2007) Palmitoylated proteins: purification and identification. *Nature Protoc.* 2, 1573–1584.

(26) Kishore, N. S., Lu, T. B., Knoll, L. J., Katoh, A., Rudnick, D. A., Mehta, P. P., Devadas, B., Huhn, M., Atwood, J. L., and Adams, S. P. et al. (1991) The substrate specificity of Saccharomyces cerevisiae myristoyl-CoA:protein N-myristoyltransferase. Analysis of myristic acid analogs containing oxygen, sulfur, double bonds, triple bonds, and/or an aromatic residue. *J. Biol. Chem.* 266, 8835–8855.

(27) Gorczyca, W. A., Gray-Keller, M. P., Detwiler, P. B., and Palczewski, K. (1994) Purification and physiological evaluation of a guanylate cyclase activating protein from retinal rods. *Proc. Natl. Acad. Sci. U.S.A.* 91, 4014–4018.

(28) Gorczyca, W. A., Van Hooser, J. P., and Palczewski, K. (1994) Nucleotide inhibitors and activators of retinal guanylyl cyclase. *Biochemistry* 33, 3217–3222.

(29) Orban, T., Bereta, G., Miyagi, M., Wang, B., Chance, M. R., Sousa, M. C., and Palczewski, K. (2010) Conformational changes in guanylate cyclase-activating protein 1 induced by Ca2+ and N-terminal fatty acid acylation. *Structure* 18, 116–126.

(30) Farazi, T. A., Waksman, G., and Gordon, J. I. (2001) Structures of Saccharomyces cerevisiae N-myristoyltransferase with bound myristoylCoA and peptide provide insights about substrate recognition and catalysis. *Biochemistry* 40, 6335–6343.

(31) Atsuzawa, K., Nakazawa, A., Mizutani, K., Fukasawa, M., Yamamoto, N., Hashimoto, T., and Usuda, N. (2010) Immunohistochemical localization of mitochondrial fatty acid beta-oxidation enzymes in Muller cells of the retina. *Histochem. Cell Biol.* 134, 565–579.

(32) Kurtz, D. M., Rinaldo, P., Rhead, W. J., Tian, L., Millington, D. S., Vockley, J., Hamm, D. A., Brix, A. E., Lindsey, J. R., Pinkert, C. A., O'Brien, W. E., and Wood, P. A. (1998) Targeted disruption of mouse

long-chain acyl-CoA dehydrogenase gene reveals crucial roles for fatty acid oxidation. *Proc. Natl. Acad. Sci. U.S.A. 95*, 15592–15597.

(33) Le, W., Abbas, A. S., Sprecher, H., Vockley, J., and Schulz, H. (2000)Long-chain acyl-CoA dehydrogenase is a key enzyme in the mitochondrial beta-oxidation of unsaturated fatty acids. *Biochim. Biophys. Acta 1485*, 121–128.

(34) Ensenauer, R., He, M., Willard, J. M., Goetzman, E. S., Corydon, T. J., Vandahl, B. B., Mohsen, A. W., Isaya, G., and Vockley, J. (2005) Human acyl-CoA dehydrogenase-9 plays a novel role in the mitochondrial beta-oxidation of unsaturated fatty acids. *J. Biol. Chem. 280*, 32309–32316.

(35) He, M., Rutledge, S. L., Kelly, D. R., Palmer, C. A., Murdoch, G., Majumder, N., Nicholls, R. D., Pei, Z., Watkins, P. A., and Vockley, J. (2007)A new genetic disorder in mitochondrial fatty acid beta-oxidation: ACAD9 deficiency. *Am. J. Hum. Genet. 81*, 87–103.

(36) Tyni, T., Paetau, A., Strauss, A. W., Middleton, B., and Kivela, T. (2004)Mitochondrial fatty acid beta-oxidation in the human eye and brain: implications for the retinopathy of long-chain 3-hydroxyacyl-CoA dehydrogenase deficiency. *Pediatr. Res. 56*, 744–750.

(37) Bazan, N. G. (2007)Homeostatic regulation of photoreceptor cell integrity: significance of the potent mediator neuroprotectin D1 biosynthesized from docosahexaenoic acid: the Proctor Lecture. *Invest. Ophthalmol. Vis. Sci. 48*, 4866–4881; biography 4864—4865.

(38) Bhatnagar, R. S., Futterer, K., Farazi, T. A., Korolev, S., Murray, C. L., Jackson-Machelski, E., Gokel, G. W., Gordon, J. I., and Waksman, G. (1998)Structure of N-myristoyltransferase with bound myristoylCoA and peptide substrate analogs. *Nat. Struct. Biol. 5*, 1091–1097.

(39) St Jules, R., Kennard, J., Setlik, W., and Holtzman, E. (1992) Frog cones as well as Muller cells have peroxisomes. *Exp. Eye Res. 54*, 1–8.

(40) Tran, T. N., and Christophersen, B. O. (2002)Partitioning of polyunsaturated fatty acid oxidation between mitochondria and peroxisomes in isolated rat hepatocytes studied by HPLC separation of oxidation products. *Biochim. Biophys. Acta 1583*, 195–204.

(41) Jayakumar, A., Tai, M. H., Huang, W. Y., al-Feel, W., Hsu, M., Abu-Elheiga, L., Chirala, S. S., and Wakil, S. J. (1995)Human fatty acid synthase: properties and molecular cloning. *Proc. Natl. Acad. Sci. U.S.A. 92*, 8695–8699.

(42) Smith, S., and Tsai, S. C. (2007)The type I fatty acid and polyketide synthases: a tale of two megasynthases. *Nat. Prod. Rep. 24*, 1041–1072.

(43) Wanders, R. J., Ruiter, J. P., L, I. J., Waterham, H. R., and Houten, S. M. (2010)The enzymology of mitochondrial fatty acid beta-oxidation and its application to follow-up analysis of positive neonatal screening results. *J. Inherit. Metab. Dis. 33*, 479–494.

(44) Ramsay, R. R., and Zammit, V. A. (2004)Carnitine acyltransferases and their influence on CoA pools in health and disease. *Mol. Aspects Med. 25*, 475–493.

(45) Eaton, S. (2002)Control of mitochondrial beta-oxidation flux. *Prog. Lipid Res. 41*, 197–239.

(46) Palczewski, K. (2006)G protein-coupled receptor rhodopsin. *Annu. Rev. Biochem. 75*, 743–767.

(47) Jastrzebska, B., Tsybovsky, Y., and Palczewski, K. (2010)Complexes between photoactivated rhodopsin and transducin: progress and questions. *Biochem. J. 428*, 1–10.

(48) Stinson, A. M., Wiegand, R. D., and Anderson, R. E. (1991) Recycling of docosahexaenoic acid in rat retinas during n-3 fatty acid deficiency. *J. Lipid Res. 32*, 2009–2017.

(49) Semple-Rowland, S. L., Gorczyca, W. A., Buczylko, J., Helekar, B. S., Ruiz, C. C., Subbaraya, I., Palczewski, K., and Baehr, W. (1996) Expression of GCAP1 and GCAP2 in the retinal degeneration (rd) mutant chicken retina. *FEBS Lett. 385*, 47–52.

(50) Johnson, W. C., Jr., Palczewski, K., Gorczyca, W. A., Riazance-Lawrence, J. H., Witkowska, D., and Polans, A. S. (1997)Calcium binding to recoverin: implications for secondary structure and membrane association. *Biochim. Biophys. Acta 1342*, 164–174.

(51) Duda, T., Goraczniak, R., Surgucheva, I., Rudnicka-Nawrot, M., Gorczyca, W. A., Palczewski, K., Sitaramayya, A., Baehr, W., and Sharma, R. K. (1996)Calcium modulation of bovine photoreceptor guanylate cyclase. *Biochemistry 35*, 8478–8482.

(52) Catala, A. (2010)A synopsis of the process of lipid peroxidation since the discovery of the essential fatty acids. *Biochem. Biophys. Res. Commun. 399*, 318–323.